

# The effect of fire and permafrost interactions on soil carbon accumulation in an upland black spruce ecosystem of interior Alaska: implications for post-thaw carbon loss

JONATHAN A. O'DONNELL\*, JENNIFER W. HARDEN†, A. DAVID MCGUIRE‡, MIKHAIL Z. KANEVSKIY§, M. TORRE JORGENSEN¶ and XIAOMEI XU||

\*Department of Biology and Wildlife, University of Alaska Fairbanks, Fairbanks, AK, USA, †US Geological Survey, Menlo Park, CA, USA, ‡US Geological Survey, Alaska Cooperative Fish and Wildlife Research Unit, University of Alaska Fairbanks, Fairbanks, AK, USA, §Institute of Northern Engineering, University of Alaska Fairbanks, Fairbanks, AK, USA, ¶Alaska Ecoscience, Fairbanks, AK, USA, ||Department of Earth System Science, University of California, Irvine, CA, USA

## Abstract

High-latitude regions store large amounts of organic carbon (OC) in active-layer soils and permafrost, accounting for nearly half of the global belowground OC pool. In the boreal region, recent warming has promoted changes in the fire regime, which may exacerbate rates of permafrost thaw and alter soil OC dynamics in both organic and mineral soil. We examined how interactions between fire and permafrost govern rates of soil OC accumulation in organic horizons, mineral soil of the active layer, and near-surface permafrost in a black spruce ecosystem of interior Alaska. To estimate OC accumulation rates, we used chronosequence, radiocarbon, and modeling approaches. We also developed a simple model to track long-term changes in soil OC stocks over past fire cycles and to evaluate the response of OC stocks to future changes in the fire regime. Our chronosequence and radiocarbon data indicate that OC turnover varies with soil depth, with fastest turnover occurring in shallow organic horizons (~60 years) and slowest turnover in near-surface permafrost (>3000 years). Modeling analysis indicates that OC accumulation in organic horizons was strongly governed by carbon losses via combustion and burial of charred remains in deep organic horizons. OC accumulation in mineral soil was influenced by active layer depth, which determined the proportion of mineral OC in a thawed or frozen state and thus, determined loss rates via decomposition. Our model results suggest that future changes in fire regime will result in substantial reductions in OC stocks, largely from the deep organic horizon. Additional OC losses will result from fire-induced thawing of near-surface permafrost. From these findings, we conclude that the vulnerability of deep OC stocks to future warming is closely linked to the sensitivity of permafrost to wildfire disturbance.

**Keywords:** boreal forest, climate change, permafrost, soil carbon, wildfire

Received 8 April 2010; revised version received 21 July 2010 and accepted 7 September 2010

## Introduction

High-latitude regions harbor large amounts of organic carbon (OC) in soil (Ping *et al.*, 2008a; Schuur *et al.*, 2008; Kuhry *et al.*, 2009; Tarnocai *et al.*, 2009). Some permafrost soils in particular began accumulating OC before the Last Glacial Maximum (Schirrmeister *et al.*, 2002). Recent climate warming at northern latitudes has resulted in warming and thawing of permafrost in many regions (Osterkamp & Romanovsky, 1999; Jorgenson *et al.*, 2001, 2006), which may mobilize OC stocks from deep soil reservoirs via decomposition, leaching, or erosion. Future warming will likely increase the fre-

quency and severity of wildfires in the boreal region (Balshi *et al.*, 2009b; Flannigan *et al.*, 2009) and consequently, may increase rates of permafrost degradation (Shur & Jorgenson, 2007). Release of OC stocks from permafrost as carbon dioxide (CO<sub>2</sub>) or methane may function as a strong positive feedback to atmospheric warming (Walter *et al.*, 2006; Schuur *et al.*, 2009).

A recent analysis suggests that the terrestrial carbon (C) sink of the boreal region may be weakening, partly in response to changes in the wildfire regime and widespread permafrost thaw (McGuire *et al.*, 2010). Previous modeling studies have quantified the influence of fire on soil C dynamics in surface organic horizons of black spruce ecosystems (Harden *et al.*, 2000; Carrasco *et al.*, 2006; Fan *et al.*, 2008), but considerable uncertainty still exists regarding the fate of deeper

Correspondence: Jonathan O'Donnell, tel. +1 907 4 55 6305, fax +1 907 474 7872, e-mail: jaodonnell@alaska.edu

C pools in unfrozen mineral soil and permafrost (Trumbore & Czimczik, 2008). Given the sensitivity of organic matter decomposition to temperature (Cox *et al.*, 2000; Davidson & Janssens, 2006), active layer depth (ALD; defined as the depth of soil above permafrost that thaws and refreezes annually) should influence decomposition rates of organic matter in mineral soil, if only by determining the proportion of OC in a thawed or frozen state. Immediately following fire, ALD typically increases due to the combustion of surface organic horizons, which insulate permafrost from warm summer air temperatures (Yi *et al.*, 2009a,b; Jorgenson *et al.*, 2010). However, recovery of surface organic horizons and the forest canopy between fire cycles can help attenuate long-term degradation of near-surface permafrost and allow recovery of the active layer to prefire depths (Yi *et al.*, 2009a,b). In this way, the sensitivity of permafrost to fire disturbance is intimately coupled to deep soil C dynamics, and in turn, to terrestrial C feedbacks to the climate system (Chapin *et al.*, 2008).

Here, we quantify soil C stocks and model long-term patterns of C storage in an upland black spruce ecosystem in interior Alaska developed on Pleistocene loess deposits that contain high-ice permafrost (yedoma; Tomirdiario *et al.*, 1984; Schirmermeister *et al.*, 2002). Our primary objectives were to (1) measure C storage in active-layer soils and deep permafrost (~20 m), (2) quantify rates of OC accumulation using both chronosequence and radiocarbon methodologies, and (3) develop a fire–C interaction model to evaluate the effects of different fire regimes on soil C storage. By integrating field observations and radiocarbon estimates of C turnover into a modeling framework, we are able to assess the interactive effects of fire and permafrost on long-term soil C storage. We also discuss the potential of permafrost thaw on post-thaw C loss from mineral soil horizons.

## Materials and methods

### Description of sites along fire/thaw chronosequence

Using aerial photography, satellite imagery, and maps of historical fire perimeters, we selected fire chronosequence sites near Hess Creek (65.56758°N, 148.92487°W, datum = NAD83), approximately 150 km north of Fairbanks, Alaska (see Supporting Information, Fig. S1). All study sites were located in forested north-facing slopes underlain by permafrost and were somewhat poorly drained, and are generally representative of black spruce ecosystems in the discontinuous permafrost zone of Alaska (e.g. Kane *et al.*, 2005) and Canada (Harden *et al.*, 1997). Study sites were located within the 2003 Erickson Creek Burn ( $n = 3$  stands), a 1993 Burn ( $n = 1$ ), a 1990 Burn ( $n = 1$ ), a 1967 Burn ( $n = 1$ ), and mature unburned stands ( $n = 3$ ; age =  $148 \pm 28$  years).

The regional climate of interior Alaska is characterized by a continental climate, with temperature extremes ranging from  $-50$  to  $35$  °C. At the Hess Creek study region, the average daily air temperature ranges from  $-25$  °C in January to  $15$  °C in July. Annual precipitation averages 270 mm, 65% of which falls during the summer growing season (mid-May to early September). The cold snow period in interior Alaska is typically >210 days long and at our sites, maximum snow accumulation (average = 44 cm; J. A. O'Donnell, unpublished results) occurred in late March.

Vegetation at each stand was described according to the Alaska Vegetation Classification System (Vioreck *et al.*, 1992). The dominant forest type on north-facing slopes of the Hess Creek region is open black spruce [*Picea mariana* (Mill.) B.S.P.]. In mature black spruce stands, the forest understory was composed of small woody shrubs, such as *Vaccinium vitis-idaea* and *Ledum groenlandicum*. Feather mosses (*Pleurozium schreberi* and *Hylocomium splendens*), sphagnum (*Sphagnum fuscum*), and reindeer lichens (*Cladonia stellaris* and *Cladonia arbuscula*) dominated ground cover in the mature black spruce stands. In the recently burned black spruce stands (2003 Erickson Creek fire), vegetation was dominated by standing dead *P. mariana*, and living *V. vitis-idaea*, *Vaccinium uliginosum*, *L. groenlandicum*, and *Equisetum* spp. Burned organic soil surfaces were quickly colonized by *Ceratodon purpureus* in the recently burned stands. The intermediate stand age (i.e. 1990 Burn, 1993 Burn) was dominated by the shrubs *Salix pulchra*, *L. groenlandicum*, and *V. vitis-idaea*. The 1990 Burn was also colonized by paper birch (*Betula neoalaskana*) and bluejoint (*Calamagrostis canadensis*). In the stands that burned in 1967, *P. mariana* and *B. neoalaskana* were the dominant tree species, *V. vitis-idaea* and *L. groenlandicum* were the dominant understory shrubs, and the feather moss *H. splendens*-dominated ground cover.

Soils at Hess Creek were classified as Gelisols, due to the presence of permafrost within 100 cm of the soil surface (USDA–NRCS). Organic soil horizons overlying mineral soil were composed of live moss, fibrous and amorphous (Oi and Oe or Oa) organic matter, and varied in thickness with stand age. Parent material across the chronosequence was composed primarily of loess silt deposited during the Late Pleistocene. Permafrost development at Hess Creek occurred in conjunction with loess sedimentation (i.e. syngenetic permafrost formation) and is commonly referred to as 'yedoma' in the literature (e.g. Tomirdiario *et al.*, 1984). We observed numerous buried organic horizons and undecomposed moss parts and rootlets in the frozen loess deposits. The thickness of frozen loess at Hess Creek varied spatially, and ranged from 1 to 26 m (based on the drilling of 62 boreholes). Volumetric ice content of permafrost at Hess Creek was high, ranging from 60% to 90%. Furthermore, massive ice wedges at some locations account for up to 30–50% of permafrost soil volume. High ice content of permafrost contributed to thaw settlement following fire at Hess Creek, and numerous thermokarst depressions have been observed.

### Soil sampling and chemical analyses

In September 2007, we dug pits and described soil horizons at each site along the chronosequence following USDA–NRCS

(Staff, 1998) and Canadian (Committee, CASC, 1998) methodologies. Common terms used for describing organic horizons included lichen, live moss, dead moss (more moss than roots), fibric (slightly decomposed, often dominated by fine roots), mesic (moderately decomposed), and humic (highly decomposed organics). Mineral soil horizons were characterized for texture and the presence of buried organic material. We sampled organic and mineral soil horizons to a minimum of 2 m from one intensive profile at each replicate stand along the chronosequence. For the 2003 Burn and Unburned Mature stands, we sampled and analyzed soil chemistry from five profiles across three stands. For the 1967, 1990, and 1993 Burn stands, we only sampled one profile because most easily accessible stands of intermediate age reburned during the massive 2004 and 2005 fire years. In addition to the intensive profiles, we dug 10 shallow pits at each stand for each age class to describe and note the depths of horizons within the soil profile as well as note the depth of the active layer. These field soil descriptions were used to estimate OC stocks in organic horizons using simple linear equations between OC concentration and organic horizon thickness (OHT) for each horizon type. These equations were based on data from two sites within interior Alaska (Manies *et al.*, 2004; K. Manies, personal communication) and one site within Canada (Manies *et al.*, 2006). For more information on these equations, see Supporting Information, Table S1.

We used a range of tools to sample different soil horizons for chemistry, bulk density, and moisture content. Organic soil horizons were sampled by hand using a variety of soil knives, scissors, and saws to ensure good volume measurements. Surface organic samples were taken in small increments (2–5 cm), depending on the horizon thickness and homogeneity of material. Mineral samples in the active layer were taken in 5–10 cm increments using small soil augers or soil knives. Near-surface permafrost (<3 m) cores were obtained using a SIPRE (Snow, Ice, and Permafrost Research Establishment) corer (7.5 cm inside diameter) with Tanaka power head. We collected a minimum of one near-surface permafrost core from each stand. Deep permafrost samples (up to 21.5 m) were collected in May 2008 in association with the State of Alaska Department of Transportation and Public Facilities (AKDOT&PF). Samples were obtained along a transect spanning both Unburned Mature and 2003 Burn stands. Hollow stem drilling was performed by AKDOT&PF with a drill rig equipped with a modified CME sampler (Central Mine Equipment Inc., St. Louis, MO, USA). Subsamples of frozen soil were collected from deep permafrost cores based on differences in visible ice content, soil texture, and the presence or absence of organic matter.

We analyzed soil samples (organic horizons, mineral soil of the active layer, near-surface and deep permafrost) for total C and nitrogen (N) using a Carlo Erba NA1500 (CE Elantech, Lakewood, NJ, USA) elemental analyzer. For organic horizon samples, where inorganic carbon (IC) is largely absent, total C represents total OC. For all mineral soil horizons, we first removed carbonates using the acid fumigation technique (Hedges & Stern, 1984; Komada *et al.*, 2008) before running samples to determine total OC concentration. Briefly, we preweighed samples in silver (Ag) capsules and transferred

them to a small desiccator. Samples were wet with 50  $\mu$ L of deionized water and then exposed to vaporous hydrochloric acid (1N) for 6 h, during which carbonates degassed from samples as CO<sub>2</sub>. We also ran mineral samples without acid fumigation to determine total C concentration. Total IC was calculated as the difference between total C and total OC. OC stocks were calculated by horizon type by multiplying OC concentration (% by mass), bulk density (oven dry), and horizon thickness. We then calculated total OC stocks to 1 m and estimated the range of OC stocks in yedoma deposits.

Organic matter and mineral soil samples from three profiles (Unburned Mature, 2003 Burn, 1967 Burn) were analyzed for radiocarbon (<sup>14</sup>C) to evaluate accumulation rates and turnover times of OC throughout the soil profile. Samples were sent to the W. M. Keck C Cycle Accelerator Mass Spectrometer (AMS) Laboratory at the University of California Irvine for analysis as described in Southon *et al.* (2004). To evaluate the effect of acid fumigation on carbonate removal, a subset of bulk mineral samples received an acid–base–acid (ABA) pretreatment, consisting of an acid wash (HCl), repeated base washes (NaOH), and one final HCl treatment followed by a rinse with deionized water. A sample of <sup>14</sup>C-free coal was also ABA treated to ensure no <sup>14</sup>C contamination during the pretreatment process. Organic matter from soil was then combusted at 900 °C in evacuated, sealed quartz tubes in the presence of cupric acid and Ag wire. Following cryogenic purification, CO<sub>2</sub> was reduced to graphite in a reaction at 500–550 °C using the sealed tube Zn reduction method (Xu *et al.*, 2007). Radiocarbon data are reported as  $\Delta^{14}\text{C}$ , or the per mil deviation of the <sup>14</sup>C/<sup>12</sup>C ratio in the sample from that of an oxalic standard that has been decay corrected to 1950 (Stuiver & Polach, 1977). The  $\Delta^{14}\text{C}$  values we report have been corrected for mass-dependent fractionation using the *in situ* simultaneous AMS  $\Delta^{13}\text{C}$  measurement.

#### *Soil C accumulation rates in organic, mineral, and permafrost soils*

We used a fire chronosequence approach to quantify rates of C accumulation in surface organic layers (Harden *et al.*, 1997) and a radiocarbon model (e.g. Trumbore & Harden, 1997) to quantify rates of C accumulation in thawed mineral soil and near-surface permafrost. For both methods, the net change in C storage (dC/dt) is governed by annual C inputs (modeled as constant  $I$ ; kg C m<sup>-2</sup> yr<sup>-1</sup>), decomposition (modeled as first order loss constant,  $k$ ; yr<sup>-1</sup>), and OC stocks in a given year [ $C(t)$ ]. The C balance for any given year is reflected in the equation:

$$dC/dt = I - kC(t). \quad (1)$$

If we assume that the initial C concentration ( $C_0$ ) is zero, solving this equation yields the following equation:

$$C(t) = (I/k) \times (1 - \exp^{-kt}). \quad (2)$$

To determine the net rate of C accumulation in surface organic horizons, we plotted recent C [ $C(t)$ ] stocks (i.e. C recovery, or C stocks above char layer in organic horizon) vs.

$t$  (as determined by chronosequence fire scars). This plot was then fit with Eqn (2) to derive estimates of  $I$  and  $k$  for shallow organic horizons between fire events. For thawed mineral soil and permafrost, we used radiocarbon data to determine the age of OC at a given depth. We then plotted cumulative OC stocks  $[C(t)]$  vs.  $t$  (as determined by radiocarbon) and fit Eqn (2) to the data to determine  $I$  and  $k$ . Trumbore & Harden (1997) used this radiocarbon method for sites dominated by moss (e.g. *Sphagnum* spp.), where vertical mixing of layers is minimal. Here, we also assume that mixing of organic matter in mineral soil is minimal. This assumption is supported by the occurrence of syngenetic permafrost, which formed in conjunction with the accumulation of sediment. However, in some soil horizons, we observed the effects of cryoturbation, which is an important mechanism of soil mixing and C burial (Bockheim, 2007; Ping *et al.*, 2008b). Our estimates of soil C accumulation in mineral soil incorporate both syngenetic aggradation and cryoturbation processes.

### Model description and development

Harden *et al.* (2000) developed a long-term C accumulation model to examine the role of wildfire on C dynamics in shallow and deep organic horizons. We modified the model to include both unfrozen and frozen mineral soil horizons (see Supporting Information for model details). To incorporate C dynamics of mineral soil into the model, we first simulated permafrost dynamics over time using the simple empirical relationship between ALD and OHT, as measured across the fire chronosequence at Hess Creek. OHT at a given time-step was calculated from OC stocks in each organic horizon ( $C_{\text{shallow}}$  and  $C_{\text{deep}}$  at time  $t$ ), following the equations of Yi *et al.* (2009a) and modified to fit our observations at Hess Creek:

$$C_{\text{sum}} = ax_{\text{sum}}^b, \quad (3)$$

where  $C_{\text{sum}}$  are the cumulative C stocks for a given horizon type,  $x_{\text{sum}}$  is the summed thickness of the horizon, and  $a$  and  $b$  are regression parameters. Summed thickness refers to the addition of multiple sample thicknesses taken from a given horizon (e.g. fibric horizon) for C analysis. For our study, we divided organic soils in three distinct horizons following the approach of Yi *et al.* (2009a): live/dead moss, fibrous organic matter, and amorphous organic matter. In our model simulations, ALD averaged between 40 and 50 cm in a mature black spruce stand and between 75 and 85 cm in a recently burned stand.

Inputs ( $I_{\text{mineral}}$ ) of C to mineral soil ( $C_{\text{mineral}}$ ) were based on Eqn (2) for thawed mineral soil at a recently burned stand (2003 Burn).  $C_{\text{mineral}}$  consists primarily of roots, char, and buried wood. Initial  $C_{\text{mineral}}$  values were determined from the simple linear relationship between cumulative C stocks and cumulative thawed mineral thickness as measured at Hess Creek [Eqn (4)]. ALD governs the proportion of  $C_{\text{mineral}}$  that is either in the seasonally thawed ( $C_{\text{active-layer}}$ ) or perennially frozen ( $C_{\text{permafrost}}$ ) state, and thus determines the rate at which  $C_{\text{mineral}}$  will decompose.  $C_{\text{active-layer}}$  decomposes at first order decay constant  $k_{\text{active-layer}}$  [as determined from Eqn (2)], while  $C_{\text{permafrost}}$  decomposes at first order decay constant  $k_{\text{permafrost}}$

[as determined from Eqn (2)]. Maximum ALD measured at Hess Creek was 84 cm from 2007 to 2009, which suggests that burn severity of recent fires was not sufficient to cause deeper thaw in this ice-rich silt. For each soil horizon, our estimates of  $I$  and  $k$  represent average input rates and turnover, respectively, and thus integrate past climatic, nutrient, and successional controls on C inputs to soil.

### Forecasting changes in deep soil

To evaluate the potential effect of future changes in the fire regime on soil C dynamics, we conducted a full factorial experiment varying fire return interval (FRI) and burn severity (SEV) and evaluated C storage in organic and mineral soil horizons. This approach allowed us to evaluate both the effects of individual factors on soil C dynamics, and also to evaluate the interaction between these two factors. For FRI, we prescribed two frequencies (120 and 80 years), based on the range of FRIs reported for other black spruce ecosystems in the boreal region (Kasischke *et al.*, 1995). We also prescribed burn severities of 64% and 77% (percentage of total organic layer depth consumed during fire), which reflect average modern burn severities for north (i.e. intermediate severity) and south-facing slopes (i.e. high severity), respectively, in interior Alaska (Kane *et al.*, 2007). In this model, SEV did not result in the direct combustion of organic matter in mineral soil or impact char inputs to mineral soil. FRI and SEV parameters were prescribed to reflect potential changes in the fire regime of black spruce ecosystems in response to future warming (e.g. Flannigan *et al.*, 2009). Because active-layer dynamics in the model were governed by our field measurements across the chronosequence, the model did not cause deep thawing of near-surface permafrost in any of the four future scenarios. To evaluate the effect of deep thawing on soil C dynamics, we ran a fifth scenario where all of the near-surface permafrost thawed with a FRI of 80 years and SEV of 77%. For each fire scenario, we ran the calibrated model up to the year 6500, at which point we shifted the fire regime and tracked OC stocks under these different fire treatments. We assume in the model that  $I$  and  $k$  values remain constant. While we recognize that this is unlikely due to sensitivity of  $I$  and  $k$  parameters to the changes in fire regime, air and soil temperature, and soil moisture, this assumption allows us to isolate the interactions among fire regime, permafrost, and deep C storage.

## Results

### Field characterization of soil properties

We observed a negative exponential relationship between ALD (cm) and OHT (cm;  $R^2 = 0.79$ ;  $P = 0.0029$ ; Fig. 1), characterized by the equation:

$$\text{ALD} = 103.7537 \times e^{(-0.0349 \times \text{OHT})}. \quad (4)$$

OHT varied across the fire chronosequence, averaging  $24 \pm 1$  cm ( $\pm$  SE) in Unburned Mature stands,

16 ± 1 cm in the 1967 burn, and 14 ± 1 cm in the 2003 Burn. ALD also varied across the fire chronosequence, averaging 45 ± 1 cm in Unburned Mature stands, 53 ± 2 cm in the 1967 Burn, and 65 ± 2 cm in the 2003 Burn.

In general, bulk density (oven dry) pooled for all chronosequence sites varied with soil horizon type (Table 1). Organic soil horizons had low bulk density values, averaging 0.05 ± 0.01 g cm<sup>-3</sup> in both live moss and fibrous horizons and 0.23 ± 0.05 g cm<sup>-3</sup> in amorphous organic horizons (Table 1). Mineral soil of the active layer (A, B, and C horizons) generally had higher mean bulk density values (1.23 ± 0.06 g cm<sup>-3</sup>) than frozen mineral soil (0.93 ± 0.02 g cm<sup>-3</sup>). This difference in

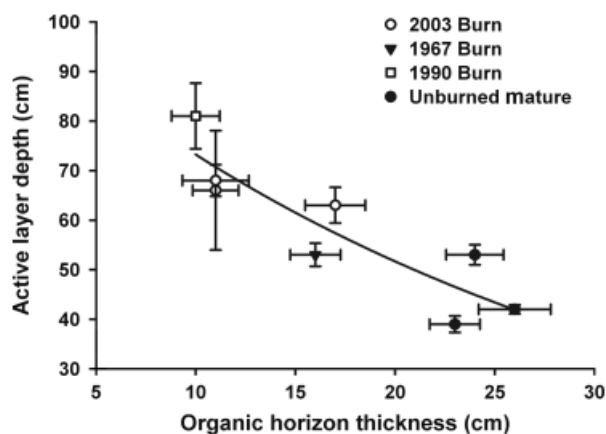


**Fig. 1** Relationship between active layer depth (ALD) and organic horizon thickness (OHT) measured across chronosequence at Hess Creek. The curve is represented by the following exponential equation:  $ALD = 103.7537 \times e^{(-0.0349 \times OHT)}$ . OHT and ALD measurements were drawn from replicate 2003 Burn ( $n = 3$ ) and Unburned Mature ( $n = 3$ ) stands, and individual 1967 Burn and 1990 Burn stands.

bulk density between frozen and thawed mineral soil can be attributed to the high volumetric ice content of syngenetic permafrost, which averaged between 66% and 78% in the top 10 m of permafrost (Table 1).

#### Soil chemistry

OC concentration averaged between 38.17 ± 1.00% in the organic soil horizons, 3.37 ± 0.68% in mineral soil of the active layer, and 1.70 ± 0.11% in permafrost when data were pooled for all sites (Table 1). Similarly, organic N averaged between 1.02 ± 0.03% in the organic horizons, and 0.15 ± 0.02% in mineral soil (active layer and permafrost). IC averaged 0.10 ± 0.07% in mineral soil of the active layer and 0.43 ± 0.03% in permafrost. In the mineral soils of the active layer, IC only accounted for 3% of total C. However, in permafrost, IC accounted for between 14% and 25% of total C. OC stocks in the Unburned Mature stand averaged 6.59 ± 2.46, 6.11 ± 3.15, and 4.43 ± 1.95 kg C m<sup>-2</sup> in the organic horizon, mineral soil of the active layer, and near-surface permafrost, respectively (Fig. 2a). In the 2003 Burn, OC stocks averaged 4.26 ± 0.65, 9.79 ± 0.80, and 4.66 ± 0.62 kg C m<sup>-2</sup> in the organic horizon, mineral soil of the active layer, and near-surface permafrost, respectively (Fig. 2a). The relationships between  $C_{sum}$  and  $x_{sum}$  for each organic horizon type are illustrated in Fig. 3a. For mineral soil in the active layer, we observed a positive linear relationship between cumulative OC stocks and the summed thickness of mineral soil horizons in the active layer (Fig. 3b), and is described by the equation:

$$C_{sum} = 0.1843x_{sum} + 0.1503, \quad (5)$$

where  $x_{sum}$  is thickness in cm and  $C_{sum}$  is OC in kg C m<sup>-2</sup> summed to that depth. OC density in deep

**Table 1** Summary of soil properties across different soil horizons

Field horizon type	Sample size	Bulk density (g cm <sup>-3</sup> )	Field VWC (%)	Organic C (%)	Organic N (%)	Inorganic C (%)
<i>Surface organic horizons</i>						
Live moss	16	0.05 ± 0.01	16 ± 4	39.8 ± 0.7	0.97 ± 0.07	nd
Fibrous	32	0.05 ± 0.01	14 ± 3	41.7 ± 1.1	0.95 ± 0.05	nd
Amorphous	25	0.23 ± 0.05	39 ± 4	35.3 ± 2.3	1.08 ± 0.06	nd
<i>Mineral soil in active layer</i>						
A/B/C	63	1.23 ± 0.06	56 ± 2	3.4 ± 0.7	0.17 ± 0.02	0.10 ± 0.07
<i>Permafrost</i>						
fC (<1m)	29	0.70 ± 0.06	78 ± 2	1.51 ± 0.23	0.10 ± 0.01	0.32 ± 0.13
fC (1–2 m)	79	0.92 ± 0.03	68 ± 1	1.32 ± 0.13	0.11 ± 0.01	0.44 ± 0.03
fC (2–5 m)	45	0.99 ± 0.04	66 ± 2	2.55 ± 0.39	0.21 ± 0.03	0.41 ± 0.05
fC (5–10 m)	59	0.91 ± 0.04	72 ± 2	1.78 ± 0.17	0.14 ± 0.01	0.56 ± 0.07
fC (10–20 m)	17	0.99 ± 0.06	72 ± 2	1.78 ± 0.27	0.13 ± 0.02	0.30 ± 0.05

Reported values reflect means ± standard error.

VWC, volumetric water content; nd, not determined.

permafrost (i.e. yedoma deposits) from all sites was relatively consistent with depth (in top 20 m), averaging  $15.48 \pm 1.02 \text{ kg C m}^{-3}$  (Fig. 2b). IC density in yedoma was considerably lower than OC density, averaging  $<5 \text{ kg m}^{-3}$  throughout the entire profile. To estimate total OC stocks, we stratified our study region into ice-rich yedoma (gravimetric moisture content = 94.9%; wedge ice volume = 34.7%; frozen loess thickness = 16–30 m) and ice-poor yedoma (gravimetric moisture content = 76.0%; wedge ice volume = 2.4%; frozen loess thickness = 9.5–12 m). Based on our estimates, OC stocks in the ice-rich region ranged between 177 and 333  $\text{kg C m}^{-2}$  (for depths 16–30 m), whereas OC stocks in the ice-poor region varied between 162 and 205  $\text{kg C m}^{-2}$  (for depths 9–12 m).

In general,  $\Delta^{14}\text{C}$  values of organic matter decreased with depth in three soil profiles along the fire chronosequence (Fig. 4), reflecting the shift from young (i.e. modern) C in shallow organic horizons, to intermediate

age C in deep organic horizons and mineral soil of the active layer, to old C stabilized in permafrost. In shallow organic horizons, we observed the incorporation of bomb-spike  $^{14}\text{C}$  into regrowing moss layers (note positive  $\Delta^{14}\text{C}$  values in Fig. 4a and b), which reflects the recent balance between C inputs from net primary productivity (NPP) and decomposition rates. We also measured  $\Delta^{14}\text{C}$  of bulk mineral samples and pieces of charred wood buried in mineral soil; however, we did not measure substantial differences in  $\Delta^{14}\text{C}$  values between them. In one soil profile, we observed a zig-zag pattern between  $\Delta^{14}\text{C}$  values and depth (Fig. 4a), which likely reflects burial of younger organic matter below older sediments through the process of cryoturbation. We used two acid fumigation treatments (ABA and acid fumigation) to remove carbonates from mineral soil samples prior  $\Delta^{14}\text{C}$  analysis. The effect of these treatments on  $\Delta^{14}\text{C}$  values of mineral soil was small, as reflected by the similarity in values across ABA, acid

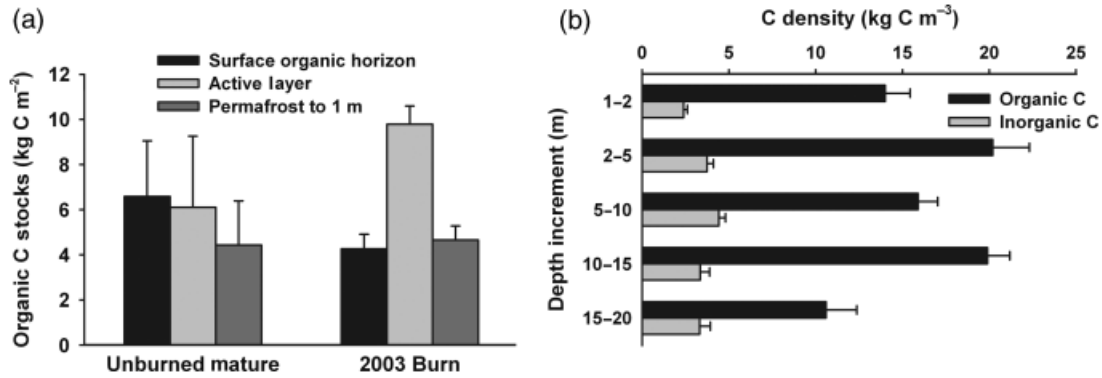


Fig. 2 (a) OC stocks in organic horizons, mineral soil of the active layer, and permafrost down to 1 m in a mature and recently burned stand. (b) OC and IC density with depth in frozen loess deposits at Hess Creek. Data are means ( $\pm 1$  standard error).

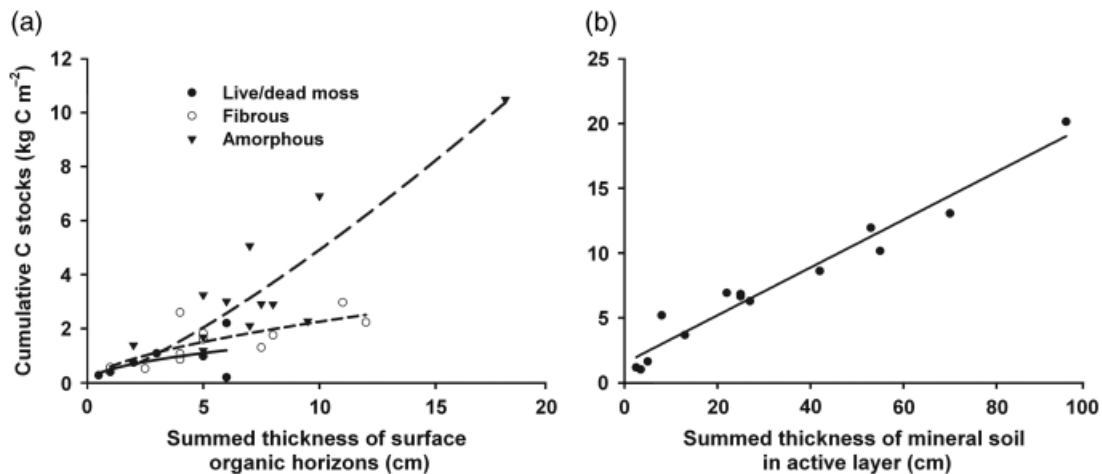
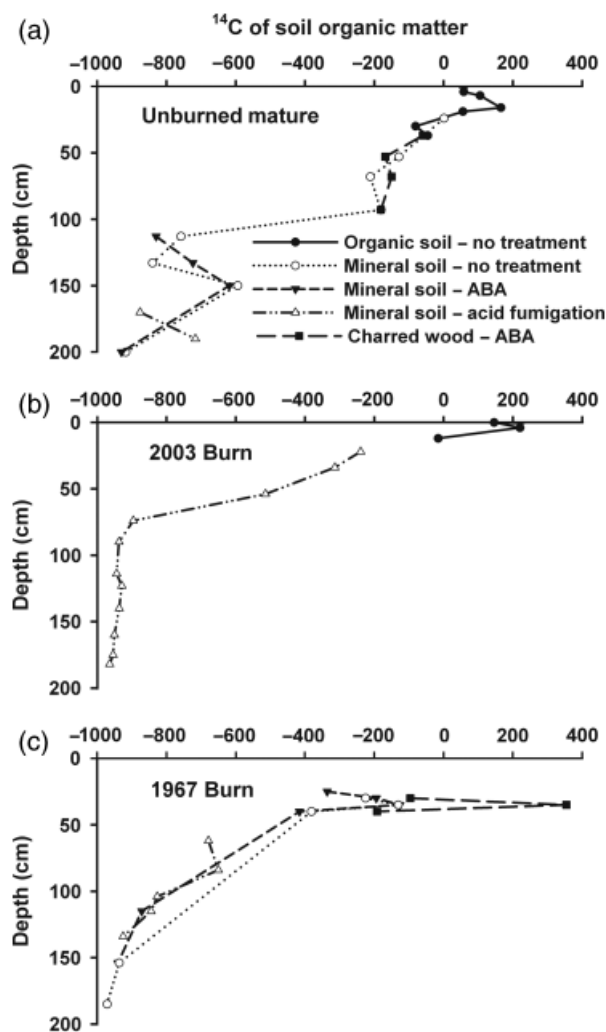


Fig. 3 Relationship between cumulative OC stocks ( $\text{kg C m}^{-2}$ ) and (a) summed thickness of individual organic horizons and (b) summed thickness of mineral horizons in the active layer ( $R^2 = 0.95$ ;  $P < 0.0001$ ). (a) Exponential curves [Eqn (3)] are fit to live/dead moss (solid line;  $a = 0.49$ ;  $b = 0.50$ ;  $R^2 = 0.27$ ;  $P = 0.19$ ), fibrous organic matter (short-dashed line;  $a = 0.59$ ,  $b = 0.59$ ;  $R^2 = 0.52$ ;  $P = 0.01$ ), and amorphous organic matter (long-dashed line;  $a = 0.26$ ;  $b = 1.27$ ;  $R^2 = 0.77$ ;  $P = 0.0002$ ).



**Fig. 4** Patterns of  $\Delta^{14}\text{C}$  of soil organic matter with depth across three stand ages near Hess Creek, Alaska. ABA refers to 'acid-base-acid' treatment, which was conducted to remove organic matter and inorganic C from the surface of soil particles.

fumigation, and untreated samples (Fig. 4a and c). This similarity suggests that the precipitation of carbonate and incorporation of organic matter were synchronous during the formation of syngenetic permafrost.

#### Rates of organic C accumulation

The rate of net C accumulation and the inputs and decomposition rates varied considerably among shallow organic horizons, mineral soil in the active layer, and mineral soil in the permafrost. In shallow organic horizons, we estimated net accumulation rate to be  $0.015 \text{ kg C m}^{-2} \text{ yr}^{-1}$ , where  $I_{\text{shallow}}$  averaged  $0.050 \pm 0.011 \text{ kg C m}^{-2} \text{ yr}^{-1}$  and  $k_{\text{shallow}}$  averaged  $0.017 \pm 0.006 \text{ yr}^{-1}$  (Fig. 5a; Table 2). To estimate  $I_{\text{mineral}}$  and  $k_{\text{active-layer}}$  we used OC and radiocarbon inventories

from the 2003 Burn, because mineral soil comprised a large proportion of active-layer soil in the recent burn stands. Net C accumulation in unfrozen mineral soil was considerably lower ( $0.002 \text{ kg C m}^{-2} \text{ yr}^{-1}$ ), as were  $I_{\text{mineral}}$  ( $0.003 \pm 0.002 \text{ kg C m}^{-2} \text{ yr}^{-1}$ ) and  $k_{\text{active-layer}}$  ( $0.0002 \pm 0.0002 \text{ yr}^{-1}$ ; Fig. 5b). For permafrost, we only used Eqn (2) for the Unburned Mature stand. For the 2003 Burn and 1967 Burn, we used simple linear accumulation, as the data did not conform to the exponential regression function (Fig. 5c). As a result, we were able to calculate inputs across all three sites, but only calculate  $k_{\text{permafrost}}$  at the unburned site.  $I_{\text{permafrost}}$  to the permafrost pool varied from 0.001 to  $0.003 \text{ kg C m}^{-2} \text{ yr}^{-1}$ . For the unburned stand, we estimated net C accumulation as  $0.001 \text{ kg C m}^{-2} \text{ yr}^{-1}$  and  $k_{\text{permafrost}}$  as  $0.0003 \pm 0.0002 \text{ yr}^{-1}$ . Also, the radiocarbon ages of organic matter in permafrost varied across sites, likely reflecting spatial differences in loess deposition rates and/or disturbance history.

#### Modeling soil C dynamics

At end of the 6500 years model run, total OC stocks varied between 17 and  $24 \text{ kg C m}^{-2}$ , depending upon the stand age (Fig. 6). Whereas OC accumulation and loss in organic horizon was driven by fire dynamics, OC stocks in mineral soil were less sensitive directly to fire and more sensitive to changes in ALD. Based on the parameterization for our model verification (see Supporting Information, Fig. S2), the OC in unfrozen mineral soil accumulated at a slow rate, with average input of  $0.003 \text{ kg C m}^{-2} \text{ yr}^{-1}$  and a turnover time of approximately 2500 years (Table 3). Permafrost OC stocks accumulated at an even slower rate, with input of  $0.003 \text{ kg C m}^{-2} \text{ yr}^{-1}$  and a turnover time of  $>3300$  years (Table 3).

After 6500 years of landform and soil development, we observed significant changes in total OC stocks in response to different changes in the fire regime. In model scenarios where permafrost only partially thawed (i.e. first four scenarios), fire caused a sharp decline in total OC stocks from 17–24 to 14–18  $\text{kg C m}^{-2}$ , depending on the treatment (Fig. 6). The low frequency, low severity (FRI = 120 years, SEV = 64%) fire treatment resulted in the smallest reduction of total OC stocks, whereas the high frequency, high severity (FRI = 80 years, SEV = 77%) fire treatment resulted in the largest reductions of total OC stocks. Based on our model, the primary losses of soil OC stocks occurred in the deep organic horizon in response to high burn severities (Fig. 7a).

Approximately 500 years after the fire regime shift, total OC stocks began to reaccumulate, with C gains outpacing losses via decomposition and fire. These C

gains were due in part to the stabilization of OC by permafrost across the first four model scenarios (Fig. 7a). To evaluate the role of near-surface permafrost as a mode of stabilizing OC, we analyzed mineral OC accumulation 'with permafrost' and 'without permafrost'. For scenarios with permafrost, we observed net increases in OC in mineral soil across all fire scenarios (Fig. 7a). For the scenario where fire-induced deeper permafrost thaw, we observed a net loss of OC from mineral soil (including both permafrost and active-layer pools). The increase in soil OC stocks in mineral soil of the active layer under the 'without permafrost' treatment reflects the transfer of thawed permafrost C to the active layer pool. From this analysis, we observed that total mineral OC stocks accumulate at a higher rate 'with permafrost' than 'without permafrost' (Fig. 7b). The difference in OC accumulation rates between treatments begins during the model spin-up (0–6500 BP) and is exacerbated following the fire regime shift, when mineral OC stocks 'without permafrost' stop accumulating OC.

## Discussion

### *C accumulation and turnover in boreal soils*

While the direct effects of wildfire and permafrost on soil OC have been the focus of much research (e.g. Bond-Lamberty *et al.*, 2007; Schuur *et al.*, 2009) the interactive effects of wildfire and permafrost have received comparatively little attention. In this study, we demonstrate that the interaction between fire and permafrost governs OC accumulation in upland forest soils of the boreal region. Fire indirectly alters OC stocks in mineral soil by reducing OHT, which in turn influences ALD (Fig. 1). In our model, ALD determines the proportion of mineral soil in a seasonally thawed (i.e. active layer) or perennially frozen (i.e. permafrost) state, and in turn, governs the susceptibility of OC in mineral soil to microbial decomposition. Our findings indicate that the presence of near-surface permafrost aids OC stabilization through the upward movement of the permafrost table between fire cycles, with ALD being driven

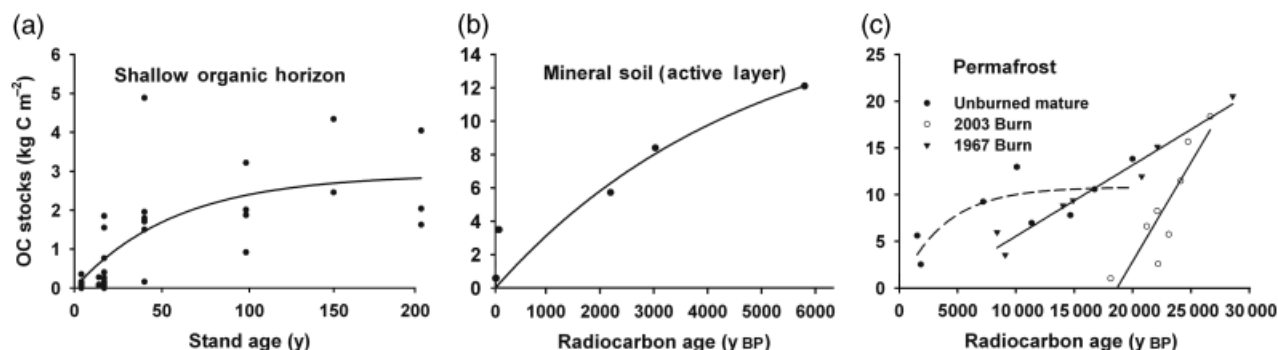


**Fig. 5** Soil OC accumulation in different soil horizons at Hess Creek. For the shallow organic horizons (a), OC stocks above char (i.e. C recovery) is plotted vs. stand age as measured across the upland fire–thaw chronosequence. Here, we fit an exponential curve [Eqn (2)] to the data following Harden *et al.* (1997) to estimate inputs (i.e. NPP) and a decay constant ( $k$ ) for the shallow organic horizon. For mineral soil in the active layer (b), OC stocks are plotted vs. radiocarbon age and fit with an exponential curve following Trumbore & Harden (1997). For permafrost (c), OC stocks are also plotted vs. radiocarbon age. The dashed line represents an exponential curve, while the solid lines represent a linear fit to the data. Inputs, decay constants and net C accumulation rates estimated from these approaches are summarized in Table 2.

**Table 2** Input and decomposition terms derived from fits of data in Fig. 5 to Eqns (1) and (2) for surface organic horizons, active layer, and permafrost

Site description	Cumulative C (kg C m <sup>-2</sup> )	Inputs (kg C m <sup>-2</sup> yr <sup>-1</sup> )	$k$ (yr <sup>-1</sup> )	Net accumulation/loss rate (kg C m <sup>-2</sup> yr <sup>-1</sup> )
<i>Recent C accumulation (organic soil above char layer)</i>				
Hess Creek Chronosequence	2.03 ± 1.08	0.050 ± 0.011	0.0173 ± 0.0056	0.015
<i>C accumulation in mineral soil of the active layer</i>				
2003 Burn	6.28 ± 4.73	0.003 ± 0.002	0.0002 ± 0.0002	0.002
<i>C accumulation in near-surface permafrost</i>				
Unburned mature	6.26 ± 4.65	0.003 ± 0.0003	0.0003 ± 0.0002	0.001
2003 Burn	10.72 ± 6.14	0.002 ± 0.0004	–	–0.001
1967 Burn	7.42	0.001 ± 0.00007	–	–0.001

Data represent mean values ± 1 standard deviation.

by ecosystem recovery and moss regrowth. Thus, disturbance by fire interacts with permafrost to create a C 'pump' from the active layer to the near-surface permafrost, effectively arresting decomposition by transferring organic matter to the 'freezer'. This finding is consistent with the short-term dynamics captured in the modeling analyses of Yi *et al.* (2010), where CO<sub>2</sub> exchange shows a net efflux immediately following fire and net uptake several years postfire.

We also illustrate that loss of permafrost following high-severity fires will result in a net loss of OC from deep mineral horizons through enhanced decomposition. These results imply that the vulnerability of deep OC stocks to future warming, and thus the magnitude of terrestrial C cycle feedbacks to the climate system from permafrost-dominated regions, is closely linked to the sensitivity of permafrost to wildfire disturbance. This finding is likely true for a wide variety of perma-

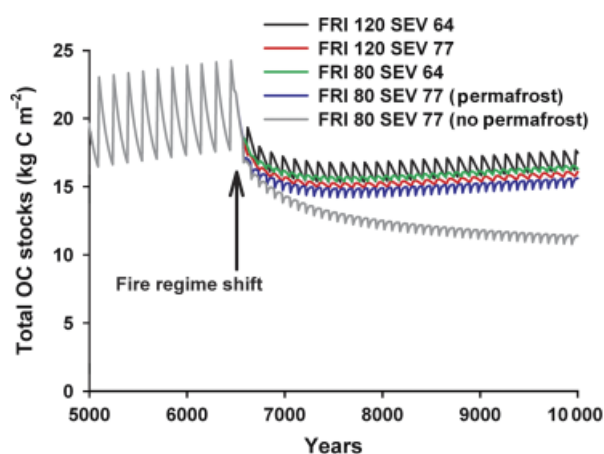


**Fig. 6** The sensitivity of total OC stocks to a change in fire regime. The five colored lines reflect different fire scenarios that vary with respect to fire return interval (FRI; 120 and 80 years) and burn severity (SEV; 64% and 77% of organic matter combusted). The gray line represents a scenario where all of the permafrost thawed following a fire regime shift (FRI 80 years, SEV 77%). FRI and SEV before the fire regime shift at year 6500 were prescribed as 150 years and 41%, respectively.

frost landscapes, although the water table and soil moisture will dictate both fire severity (and in response ALD) and rates of regeneration. For example, postfire reduction of organic horizons and increase in ALD can greatly lower the water table in well-drained black spruce stands, enhancing decomposition immediately following fire (Yi *et al.*, 2010). In poorly drained black spruce stands, however, water table depth and decomposition tend to remain relatively stable across fire cycles (Yi *et al.*, 2010).

Mineral soils in black spruce ecosystems receive OC from a variety of sources, including roots, char, humic organic matter, and leaching of dissolved organic matter. Our estimates of OC input rates to mineral soil ( $0.003 \text{ kg C m}^{-2} \text{ yr}^{-1}$ ; Table 2), as determined by the radiocarbon methodology, are lower than rates measured in other systems ( $0.019\text{--}0.026 \text{ kg C m}^{-2} \text{ yr}^{-1}$ ; Richter *et al.*, 1999). Richter *et al.* (1999) directly measured C inputs to mineral soil in a temperate forest. The difference between C inputs to mineral soil of a temperate and boreal forest was likely driven by variation in forest productivity between biomes (Jobbagy & Jackson, 2000), and by access of roots to mineral substrate. In permafrost systems, such access is limited by soil temperature and water state. Cryoturbation is another mechanism for incorporating soil C into mineral soil and permafrost at high latitudes (Michaelson *et al.*, 1996; Bockheim, 2007), particularly mixing associated with the movement of fluid materials during thawing of ice-rich permafrost (Swanson *et al.*, 1999). We observed evidence of cryoturbated horizons in a number of soil profiles (e.g. Fig. 4a). Many studies have suggested that cryoturbation activity increases with warming (see review by Bockheim, 2007), but it is unclear how fire might influence rates of C burial by cryoturbation. Our estimates of OC input to the permafrost pool (Table 2) likely reflect a range of processes, including cryoturbation, the burial of OC through a rise of the permafrost table as a result of sedimentation (i.e. syngenetic permafrost aggradation), and OC incorporation into the permafrost pool in response to the upward movement

**Table 3** Parameters used in fire–permafrost interaction model derived from field data (Table 2) and model calibration (Supporting Information Figs S2 and S3)

Model parameters	Description	Units	Model input	Sources
$I_{\text{shallow}}$	Inputs to shallow organic horizon	$\text{kg C m}^{-2} \text{ yr}^{-1}$	0.06	Hess Creek chronosequence
$k_{\text{shallow}}$	Decay constant for shallow organic horizon	$\text{yr}^{-1}$	0.024	Hess Creek chronosequence
$k_{\text{deep}}$	Decay constant for deep organic horizon	$\text{yr}^{-1}$	0.0025	Model validation from this study
$I_{\text{mineral}}$	Inputs to mineral horizons	$\text{kg C m}^{-2} \text{ yr}^{-1}$	0.003	<sup>14</sup> C accumulation model
$k_{\text{active-layer}}$	Decay constant for thawed mineral horizons	$\text{yr}^{-1}$	0.0004	<sup>14</sup> C accumulation model
$k_{\text{permafrost}}$	Decay constant for permafrost	$\text{yr}^{-1}$	0.0003	<sup>14</sup> C accumulation model
FRI	Fire return interval	year	150	Mature stand ages at Hess Creek
SEV	Burn severity	%	41	Harden <i>et al.</i> (1997)

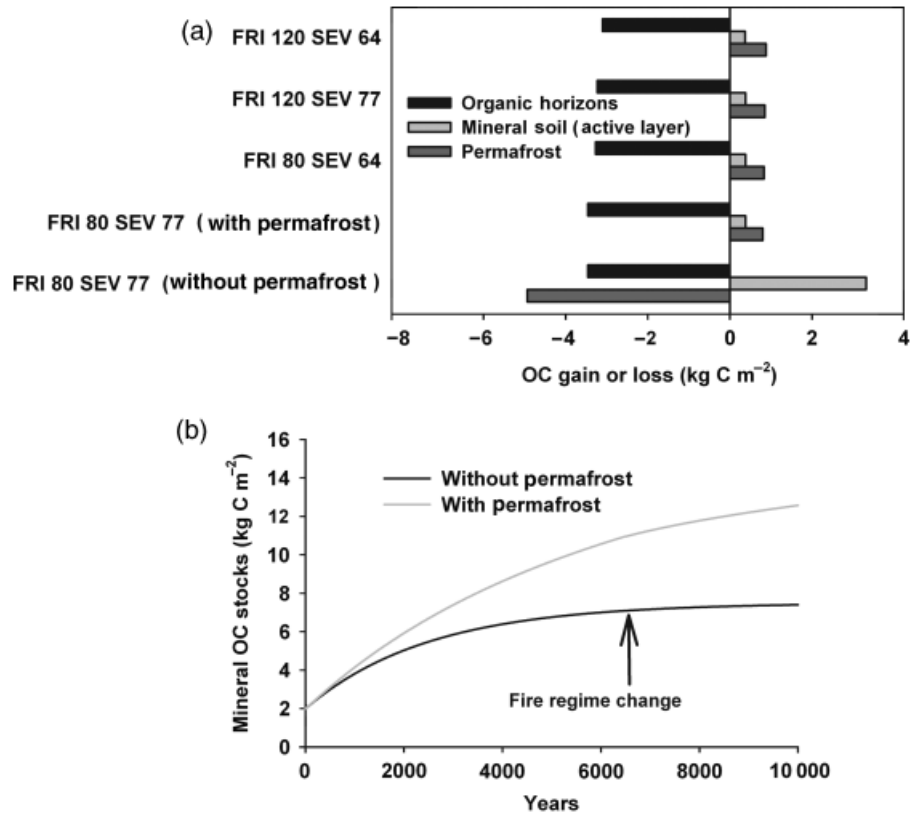


**Fig. 7** (a) Changes in OC storage across five model scenarios with contrasting fire regimes. Values reflect the difference in average OC storage after the fire regime shift (years 6500–10 000) relative to average OC stocks during the last fire cycle of the spin-up (years 6350–6500). A positive value indicates a net OC gain, while a negative value reflects a net OC loss. (b) Comparison of mineral OC accumulation between a fire scenario with near-surface permafrost and when near-surface permafrost completely thaws.

of the permafrost table between fires (i.e. quasi-syngenic permafrost aggradation).

Decomposition of organic matter in mineral soil was influenced by ALD, which determined the proportion of OC in unfrozen mineral soil of the active layer vs. near-surface permafrost. While our field data suggested that  $k_{\text{active-layer}}$  and  $k_{\text{permafrost}}$  were not significantly different (Table 2), a model calibration procedure indicated that turnover times were slightly faster in unfrozen active-layer soil (2500 years) than in permafrost (3300 years; Table 3, Supporting Information, Fig. S3). These turnover times determined through model calibration were consistent with turnover times determined through radiocarbon methodology. Furthermore, these findings are consistent with previous studies, which have documented faster decomposition rates in unfrozen soil than in frozen soil (Mikan *et al.*, 2002; Dioumaeva *et al.*, 2003). In addition to the direct effects of temperature, slower rates of decomposition in near-surface permafrost are likely due to low unfrozen water content (Romanovsky & Osterkamp, 2000; Schimel & Mikan, 2005) and low microbial abundance and activity relative to active-layer soils (Waldrop *et al.*, 2010). Our

model simulations show that the transfer of OC from the active layer to the permafrost pool is critical for lessening OC losses via decomposition and increasing net accumulation rates in mineral soil across fire cycles.

We also observed large quantities of OC buried in deep loess deposits (i.e. yedoma; Fig. 2b). OC density in yedoma averaged  $15.4 \pm 0.8 \text{ kg C m}^{-3}$  across the study area, consistent with values reported by other researchers (Dutta *et al.*, 2006; Khvorostyanov *et al.*, 2008; Ping *et al.*, 2008a; Schuur *et al.*, 2008). Yedoma sampling at Hess Creek revealed striking spatial variability in loess thickness, wedge ice volume, and segregated ice volume (Shur *et al.*, 2010), which can greatly influence estimates of OC stocks. By stratifying our study area into ice-rich and ice-poor sections, we were better able to address the impact of ground ice on OC stocks. OC accumulation rates in permafrost varied among three profiles, which may reflect spatial variation in loess deposition, OC inputs or OC losses via decomposition from permafrost. In two profiles (2003 Burn and 1967 Burn), accumulation rates were linear, suggesting that decomposition rates were low relative to OC inputs. In a third profile (Unburned Mature), OC accumulation

decreased with radiocarbon age, reflecting an increase in decomposition relative to OC inputs over time.

#### *Implications of future changes in climate, fire regime, and permafrost stability*

A number of recent studies have reported that future climate warming will likely increase fire activity in the boreal region (Gillett *et al.*, 2004; Duffy *et al.*, 2005; Balshi *et al.*, 2009b; Flannigan *et al.*, 2009). The vulnerability of permafrost to fire will likely depend most on changes in burn severity (Fig. 6; Jorgenson *et al.*, 2010) but also on fire frequency and rates of ecosystem recovery between fire events (Shur & Jorgenson, 2007). Based on our modeling results, a shift in fire regime to both more frequent and higher severity fires would cause the most significant response, with a shift from a net C sink to a net C source to the atmosphere, primarily due to OC losses from deep organic horizons (Fig. 7a). Additional OC losses may occur if near-surface permafrost completely degrades, mobilizing old permafrost C. The results of these modeling analyses could inform future investigations in boreal ecosystems underlain by permafrost, particularly those experiencing climate-driven changes in the fire regime (Kasischke & Turetsky, 2006; Flannigan *et al.*, 2009). Furthermore, similar responses to fire might be possible in response to tundra fires in the continuous permafrost zone (e.g. Jones *et al.*, 2009).

Meanwhile, future increases in NPP could offset soil OC losses from changes in the fire regime and subsequent permafrost thaw. To estimate how much NPP would have to increase to maintain current ecosystem C budget, we calculated the difference between mean OC stocks during the last fire cycle of the model spin-up (6350–6500 years) and mean OC stocks after the next three fire cycles after the fire regime shift at 6500 years. Our calculations suggest that moss and tree NPP would collectively have to increase by 7–14% in the next two to three centuries in order to offset soil C losses. Recent studies suggest that NPP of the boreal region may indeed increase in response to increased temperature, CO<sub>2</sub> fertilization, N availability, and increased fire frequency (Peng & Apps, 1999; Balshi *et al.*, 2009a). Recent findings suggest that permafrost thaw may increase soil N availability (Schuur *et al.*, 2007), which if within the rooting zone can partially offset OC losses from recently thawed soil (Schuur *et al.*, 2009). Furthermore, severe fires can result in the conversion of black spruce forests to deciduous stands (Johnstone *et al.*, 2009), which tend to have higher rates of NPP (Bond-Lamberty *et al.*, 2007). However, conversion to deciduous stands will likely reduce soil OC storage through the loss of thick organic horizons and permafrost. Together with our findings, these studies suggest that while productivity

may increase in the future, soil C turnover may also increase, resulting in a reduction of C storage in soils.

ALD is also a function of summer air temperatures, precipitation, snow depth, and soil thermal properties (Romanovsky & Osterkamp, 2000; Yoshikawa *et al.*, 2003; Nowinski *et al.*, 2010). However, we calculated ALD as a direct function of OHT and thus, values were constrained by our field measurements across the fire chronosequence at our site and in today's climate (Fig. 1). Fire did not cause deep thawing (>1 m) of near-surface permafrost, perhaps due to low fire severities (Yoshikawa *et al.*, 2003), the presence of an ice-rich intermediate layer requiring high latent heat for thawing (Shur *et al.*, 2005), and/or the location of chronosequence sites on relatively cold, wet, north-facing slopes (Swanson, 1996). However, Viereck *et al.* (2008) observed deep thawing of permafrost in an open black spruce stand following a fire near Fairbanks, with a maximum thaw depth of 302 cm 24 years after the fire. Future fire regimes, together with warmer air temperatures, may result in similar deep thawing of permafrost at Hess Creek. To more accurately assess the future response of ALD to fire and air temperature, permafrost dynamics should be simulated using numerical- (e.g. Marchenko *et al.*, 2008) or process-based thermal models (e.g. Yi *et al.*, 2009b).

Finally, soil C dynamics are sensitive to changes in temperature and moisture (Lloyd & Taylor, 1994; Davidson & Janssens, 2006), and consequently, model parameters (e.g.  $l$ ,  $k$ ) should reflect these dynamics. Yi *et al.* (2010) show that immediately following fire, increased soil temperatures and ALD enhance decomposition and inorganic N availability to plants, which results in increased NPP in early successional stands. However, in mid-successional stands, decreased ALD and cooler soils lower decomposition rates, inorganic N availability, and rates of NPP (Yi *et al.*, 2010). Kane & Vogel (2009) report that soil OC storage decreased by nearly 50% with increasing temperature (from 100 to 900 soil degree-days), presumably due to the increased rates of decomposition at higher temperatures. In a synthesis of ecosystem warming experiments, above-ground NPP and soil respiration increased by similar magnitudes to sustained warming across biomes (Rustad *et al.*, 2001). However, there is still uncertainty regarding the comparative response of NPP and soil respiration to warming in the boreal region, where sensitivity analyses are complicated by fire disturbance and the presence of permafrost (Zhuang *et al.*, 2003). In our model, decay constants ( $k$ ) integrate the 'apparent' sensitivity of decomposition to temperature and moisture during past environmental conditions as measured in the field. However, model forecasting needs to address the response of decomposition to future warming

and moisture dynamics. Thus, future simulation of soil C dynamics in our model is limited by our ability to predict the response of  $I$  and  $k$  to future climatic conditions. In the boreal region, researchers have conducted short-term incubations to estimate temperature response quotients ( $Q_{10}$ ) of decomposition across a range of organic matter substrates (Wickland & Neff, 2007; Waldrop *et al.*, 2010), which have aided parameterization of soil C models (Carrasco *et al.*, 2006; Fan *et al.*, 2008). However, because soil C storage is a function of both inputs and losses, changes in OC stocks will also depend upon production and the response of plants to future warming (Heimann & Reichstein, 2008; Balshi *et al.*, 2009a).

## Conclusion

Wildfire in the boreal region will likely exacerbate rates of permafrost thaw, but to date, has not been incorporated into climate models used for predicting loss of permafrost. Loss of permafrost will enhance decomposition and loss of organic matter stocks from both organic and mineral soil layers, accelerating feedbacks from terrestrial ecosystems to the climate system. Such feedbacks invoke a soil C loss that is transient for hundreds of years, after which time C accumulates slowly in permafrost layers. For context, we estimate that net primary production would have to increase by up to 14% relative to present-day rates following permafrost thaw in order for current C budgets to be maintained over such a regime shift.

## Acknowledgements

The authors would like to thank Stephanie Ewing for her assistance in the field and for sharing in many insightful discussions about permafrost. Many thanks also go to Pedro Rodriguez for field/laboratory assistance, Kristen Manies for assistance with data management, Yuri Shur for initiating collaborations with AKDOT&PF, and Tom Douglas for sharing laboratory space. Vladimir Romanovsky, Yuri Shur, Eran Hood, and Evan Kane provided valuable comments on an earlier version of this manuscript. Funding and support for J. O'Donnell was provided by the National Science Foundation grant EAR-0630249 and the Institute of Northern Engineering at the University of Alaska Fairbanks. The study was also supported by grants from the US Geological Survey to Harden and McGuire, and by the Bonanza Creek LTER (Long-Term Ecological Research) Program, funded jointly by NSF (grant DEB-0423442) and the USDA Forest Service (Pacific Northwest Research Station grant PNW01-JV11261952-231).

## References

- Balshi MS, McGuire AD, Duffy P, Flannigan M, Kicklighter DW, Melillo J (2009a) Vulnerability of carbon storage in North American boreal forests to wildfires during the 21st century. *Global Change Biology*, **15**, 1491–1510.
- Balshi MS, McGuire AD, Duffy P, Flannigan M, Walsh J, Melillo J (2009b) Assessing the response of area burned to changing climate in western boreal North America using a Multivariate Adaptive Regression Splines (MARS) approach. *Global Change Biology*, **15**, 578–600, doi: 10.1111/j.1365-2486.2008.01679.x.
- Boekheim JG (2007) Importance of cryoturbation in redistributing organic carbon in permafrost-affected soils. *Soil Science Society of America Journal*, **71**, 1335–1342.
- Bond-Lamberty B, Peckham SD, Ahl DE, Gower ST (2007) Fire as the dominant driver of central Canadian boreal forest carbon balance. *Nature*, **450**, 89–92.
- Carrasco JJ, Neff JC, Harden JW (2006) Modeling physical and biogeochemical controls over carbon accumulation in a boreal forest soil. *Journal of Geophysical Research*, **111**, G02004, doi: 10.1029/2005JG000087.
- Chapin FS III, Randerson JT, McGuire AD, Foley JA, Field CB (2008) Changing feedbacks in the climate–biosphere system. *Frontiers in Ecology and the Environment*, **6**, 313–320, doi: 10.1890/080005.
- Committee, CASC (1998) *The Canadian System of Soil Classification*. NRC Canada Research Press, ON, Canada pp. 1–187.
- Cox PM, Betts RA, Jones CD, Spall SA, Totterdell IJ (2000) Acceleration of global warming due to carbon-cycle feedbacks in a coupled climate model. *Nature*, **408**, 184–187.
- Davidson EA, Janssens IA (2006) Temperature sensitivity of soil carbon decomposition and feedbacks to climate change. *Nature*, **440**, 165–173.
- Dioumaeva I, Trumbore S, Schuur EAG, Goulden ML, Litvak M, Hirsch AI (2003) Decomposition of peat from upland boreal forest: temperature dependence and source of respired carbon. *Journal of Geophysical Research*, **108**, doi: 10.1029/2001JD000848.
- Duffy PA, Walsh JE, Graham JM, Mann DH, Rupp TS (2005) Impacts of large scale atmospheric-ocean variability on Alaskan fire season severity. *Ecological Applications*, **15**, 1317–1330.
- Dutta K, Schuur EAG, Neff JC, Zimov SA (2006) Potential carbon release from permafrost soils of Northeastern Siberia. *Global Change Biology*, **12**, 2336–2351, doi: 10.1111/j.1365-2486.2006.01259.x.
- Fan Z, Neff JC, Harden JW, Wickland KP (2008) Boreal soil carbon dynamics under a changing climate: a model inversion approach. *Journal of Geophysical Research*, **113**, G04016, doi: 10.1029/2008JG000723.
- Flannigan M, Stocks B, Turetsky M, Wotton M (2009) Impacts of climate change on fire activity and fire management in the circumboreal forest. *Global Change Biology*, **15**, 549–560, doi: 10.1111/j.1365-2486.
- Gillett NP, Weaver AJ, Zwiers FW, Flannigan MD (2004) Detecting the effect of climate change on Canadian forest fires. *Geophysical Research Letters*, **31**, L18211, doi: 10.1029/2004GL020876.
- Harden JW, O'Neill KP, Trumbore SE, Veldhuis H, Stocks BJ (1997) Moss and soil contributions to the annual net carbon flux of a maturing boreal forest. *Journal of Geophysical Research*, **102**, 28805–28816.
- Harden JW, Trumbore SE, Stocks BJ, Hirsch A, Gower ST, O'Neill KP, Kasischke ES (2000) The role of fire in the boreal carbon budget. *Global Change Biology*, **6** (Suppl. 1), 174–184.
- Hedges JL, Stern JH (1984) Carbon and nitrogen determinations of carbonate-containing solids. *Limnology and Oceanography*, **29**, 657–663.
- Heimann M, Reichstein M (2008) Terrestrial ecosystem carbon dynamics and climate feedbacks. *Nature*, **451**, 289–292.
- Jobbagy EC, Jackson RB (2000) The vertical distribution of soil organic carbon and its relation to climate and vegetation. *Ecological Applications*, **10**, 423–436.
- Johnstone JF, Hollingsworth TN, Chapin FS III, Mack MC (2009) Changes in fire regime break the legacy lock on successional trajectories in Alaskan boreal forest. *Global Change Biology*, **16**, 1281–1295, doi: 10.1111/j.1365-2486.2009.02051.x.
- Jones BM, Kolden CA, Jandt R, Abatzoglou JT, Urban F, Arp CD (2009) Fire behavior, weather, and burn severity of the 2007 Anaktuvuk River tundra fire, North Slope Alaska. *Arctic, Antarctic, and Alpine Research*, **41**, 309–316.
- Jorgenson MT, Racine CH, Walters JC, Osterkamp TE (2001) Permafrost degradation and ecological changes associated with a warming climate in central Alaska. *Climatic Change*, **48**, 551–579.
- Jorgenson MT, Romanovsky VE, Harden J, O'Donnell JA, Schuur EAG, Kanevskiy M (2010) Resilience and vulnerability of permafrost to climate change. *Canadian Journal of Forest Research*, **40**, 1219–1236.
- Jorgenson MT, Shur YL, Pullman ER (2006) Abrupt increase in permafrost degradation in Arctic Alaska. *Geophysical Research Letters*, **33**, L02503, doi: 10.1029/2005GL024960.
- Kane ES, Kasischke ES, Valentine DW, Turetsky MR, McGuire AD (2007) Topographic influences on wildfire consumption of soil organic carbon in interior Alaska: implications for black carbon accumulation. *Journal of Geophysical Research*, **112**, G03017, doi: 10.1029/2007JG000458.
- Kane ES, Valentine DW, Schuur EAG, Dutta K (2005) Soil carbon stabilization along climate and stand productivity gradients in black spruce forests of interior Alaska. *Canadian Journal of Forest Research*, **35**, 2118–2129.
- Kane ES, Vogel JG (2009) Patterns of total ecosystem carbon storage with changes in soil temperature in boreal black spruce forests. *Ecosystems*, **12**, 322–335, doi: 10.1007/s10021-008-9225-1.

- Kasischke ES, Christensen NL, Stocks BJ (1995) Fire, global warming, and the carbon balance of boreal forests. *Ecological Applications*, **5**, 437–451.
- Kasischke ES, Turetsky MR (2006) Recent changes in the fire regime across the North American boreal region – spatial and temporal patterns of burning across Canada and Alaska. *Geophysical Research Letters*, **33**, L09703, doi: 10.1029/2006GL025677.
- Khvorostyanov DV, Krinner G, Ciais P, Heimann M, Zimov SA (2008) Vulnerability of permafrost carbon to global warming. Part I: model description and role of heat generated by organic matter decomposition. *Tellus B*, **60**, 250–264, doi: 10.1111/j.1600-0889.2007.00333.x.
- Komada T, Anderson MR, Dormeier CL (2008) Carbonate removal from coastal sediments for the determination of organic carbon and its isotopic signatures,  $\delta^{13}\text{C}$  and  $\Delta^{14}\text{C}$ : comparison of fumigation and direct acidification by hydrochloric acid. *Limnology and Oceanography: Methods*, **6**, 254–262.
- Kuhry P, Ping CL, Tarnocai C, Schuur EAG, Zimov S (2009) Report from the international permafrost association: carbon pools in permafrost regions. *Permafrost and Periglacial Processes*, **20**, 229–234.
- Lloyd J, Taylor JA (1994) On the temperature dependence of soil respiration. *Functional Ecology*, **8**, 315–323.
- Manies KL, Harden JW, Silva SR, Briggs PH, Schmidet BM (2004) Soil data from *Picea mariana* stands near Delta Junction, AK of different stand ages and soil drainage type. US Geological Survey Open File Report, 2004-1271, pp. 1–19.
- Manies KL, Harden JW, Veldhuis H (2006) Soil data from a moderately well and somewhat poorly drained fire chronosequence near Thompson, Manitoba, Canada. US Geological Survey Open File Report, 2006-1291, pp. 1–17.
- Marchenko S, Romanovsky V, Tipenko G (2008) Numerical modeling of spatial permafrost dynamics in Alaska. In: *Proceedings of the Ninth International Conference on Permafrost, July 29–July 3, 2008* (eds Kane DL, Hinkel KM), pp. 1–6. Institute of Northern Engineering, University of Alaska Fairbanks, Fairbanks, AK.
- McGuire AD, Hayes DJ, Kicklighter DW *et al.* (2010) An analysis of the carbon balance of the Arctic Basin from 1997 to 2006. *Tellus B*, **62B**, 455–474.
- Michaelson GJ, Ping CL, Kimble JM (1996) Carbon storage and distribution in tundra soils of arctic Alaska. *Arctic and Alpine Research*, **28**, 414–424.
- Mikan CJ, Schimel JP, Doyle AP (2002) Temperature controls of microbial respiration in arctic tundra soils above and below freezing. *Soil Biology and Biochemistry*, **34**, 1785–1795.
- Nowinski NS, Taneva L, Trumbore SE, Welker JM (2010) Decomposition of old organic matter as a result of deeper active layers in a snow depth manipulation experiment. *Oecologia*, **163**, 785–792.
- Osterkamp TE, Romanovsky VE (1999) Evidence for warming and thawing of discontinuous permafrost in Alaska. *Permafrost and Periglacial Processes*, **10**, 17–37.
- Peng C, Apps MJ (1999) Modelling the response of net primary productivity (NPP) of boreal forest ecosystems to changes in climate and fire disturbance regimes. *Ecological Modelling*, **122**, 175–193.
- Ping CL, Michaelson GJ, Jorgenson MT, Kimble JM, Epstein H, Romanovsky VE, Walker DA (2008a) High stocks of soil organic carbon in the North American Arctic region. *Nature Geoscience*, **1**, 615–619, doi: 10.1038/ngeo284.
- Ping CL, Michaelson GJ, Kimble JM, Romanovsky VE, Shur YL, Swanson DK, Walker DA (2008b) Cryogenesis and soil formation along a bioclimate gradient in Arctic North America. *Journal of Geophysical Research*, **113**, G03S12, doi: 10.1029/2008JG000744.
- Richter DD, Markewitz D, Trumbore SE, Wells CG (1999) Rapid accumulation and turnover of soil carbon in re-establishing forest. *Nature*, **400**, 56–58.
- Romanovsky VE, Osterkamp TE (2000) Effects of unfrozen water on heat and mass transport processes in the active layer and permafrost. *Permafrost and Periglacial Processes*, **11**, 219–239.
- Rustad LE, Campbell JLGCTE-NEWS *et al.* (2001) A meta-analysis of the response of soil respiration, net nitrogen mineralization, and aboveground plant growth to experimental warming. *Oecologia*, **126**, 543–562, doi: 10.1007/s004420000544.
- Schimel DS, Braswell BH, Holland EA, McKeown R, Ojima DS, Painter TH, Parton WJ, Townsend AR (1994) Climatic, edaphic, and biotic controls over storage and turnover of carbon in soils. *Global Biogeochemical Cycles*, **8**, 279–293.
- Schimel JP, Mikan C (2005) Changing microbial substrate use in Arctic tundra soils through a freeze–thaw cycle. *Soil Biology and Biochemistry*, **37**, 1411–1418.
- Schirmerster L, Siegert C, Kuznetsova T *et al.* (2002) Paleoenvironmental and paleoclimatic records from permafrost deposits in the Arctic region of Northern Siberia. *Quaternary International*, **89**, 97–118.
- Schuur EAG, Bockheim J, Canadell JG *et al.* (2008) Vulnerability of permafrost carbon to climate change: implications for the global carbon cycle. *Bioscience*, **58**, 701–714.
- Schuur EAG, Crummer KG, Vogel JG, Mack MC (2007) Plant species composition and productivity following permafrost thaw and thermokarst in Alaskan tundra. *Ecosystems*, **10**, 208–292, doi: 10.1007/s10021-007-9024-0.
- Schuur EAG, Vogel JG, Crummer KG, Lee H, Sickman JO, Osterkamp TE (2009) The effect of permafrost thaw on old carbon release and net carbon exchange from tundra. *Nature*, **459**, 556–559, doi: 10.1038/nature08031.
- Shur Y, Hinkel KM, Nelson FE (2005) The transient layer: implications for geocryology and climate-change science. *Permafrost and Periglacial Processes*, **16**, 5–17.
- Shur YL, Jorgenson MT (2007) Patterns of permafrost formation and degradation in relation to climate and ecosystems. *Permafrost and Periglacial Processes*, **18**, 7–19.
- Shur YL, Kanevskiy M, White DM, Connor B (2010) Geotechnical investigations for the Dalton Highway Innovation Project as a case study of the ice-rich syngenetic permafrost. AUTC assigned project #207122, February 25, 2010.
- Southon J, Santos G, Druffel-Rodriguez K *et al.* (2004) The Keck carbon cycle AMS laboratory, University of California Irvine: initial operation and background surprise. *Radiocarbon*, **46**, 41–49.
- Staff SS (1998) *Keys to Soil Taxonomy*. Pocahontas Press Inc., Blacksburg, VA.
- Stuiver M, Polach HA (1977) Discussion: reporting of  $^{14}\text{C}$  data. *Radiocarbon*, **19**, 355–363.
- Swanson DK (1996) Susceptibility of permafrost soils to deep thaw after forest fires in interior Alaska, USA. *Arctic and Alpine Research*, **28**, 217–227.
- Swanson DK, Ping CL, Michaelson GJ (1999) Diapirism in soils due to thaw of ice-rich material near the permafrost table. *Permafrost and Periglacial Processes*, **10**, 349–367.
- Tarnocai C, Canadell JG, Schuur EAG, Kuhry P, Mahitova G, Zimov S (2009) Soil organic carbon pools in the northern circumpolar permafrost region. *Global Biogeochemical Cycles*, **23**, GB2023, doi: 10.1029/2008GB003327.
- Tomirdiaro SV, Arslanov KA, Chernenkiy BI, Tertychnaya TV, Prokhorova TN (1984) New data on formation of loess-ice sequences in Northern Yakutia and ecological conditions of mammoth fauna in the Arctic during the late Pleistocene. *Reports Academy of Sciences USSR*, **278**, 1446–1449 (in Russian).
- Trumbore SE, Czimeczik CI (2008) An uncertain future for soil carbon. *Science*, **321**, 1455–1456.
- Trumbore SE, Harden JW (1997) Accumulation and turnover of carbon in organic and mineral soils of the BOREAS northern study area. *Journal of Geophysical Research*, **102**, 28817–28830.
- Viereck LA, Dyrness CT, Batten AR, Wenzlick KJ (1992) *The Alaska vegetation classification*. General Technical Report PNW-GTR-286, US Department of Agriculture, Forest Service, Pacific Northwest Research Station.
- Viereck LA, Werdin-Pfisterer NR, Adams PC, Yoshikawa K (2008) Effect of wildfire and fireline construction on the annual depth of thaw in a black spruce permafrost forest in interior Alaska: a 36-year record of recovery. In: *Proceedings of the Ninth International Conference on Permafrost, July 29–July 3, 2008* (eds Kane DL, Hinkel KM), pp. 1845–1850. Institute of Northern Engineering, University of Alaska Fairbanks, Fairbanks, AK.
- Waldrop MP, Wickland K, White R III, Berhe AA, Harden J, Romanovsky V (2010) Molecular investigations into a globally important carbon pool: permafrost-protected carbon in Alaskan soils. *Global Change Biology*, **16**, 2543–2554.
- Walter KM, Zimov SA, Chanton JP, Verbyla D, Chapin FS III (2006) Methane bubbling from Siberian thaw lakes as a positive feedback to climate warming. *Nature*, **443**, 71–75.
- Wickland KP, Neff JC (2007) Decomposition of soil organic matter from boreal black spruce forest: environmental and chemical controls. *Biogeochemistry*, **87**, 29–47.
- Xu X, Trumbore SE, Zheng S, Southon JR, McDuffee KE, Luttgen M, Liu JC (2007) Modifying a sealed tube zinc reduction method for preparation of AMS graphite targets: reducing background and attaining high precision. *Nuclear Instruments and Methods in Physics Research B*, **259**, 320–329.
- Yi S, Manies K, Harden J, McGuire AD (2009a) Characteristics of organic soil in black spruce forests: implications for the application of land surface and ecosystem models in cold regions. *Geophysical Research Letters*, **36**, L05501, doi: 10.1029/2008GL037014.
- Yi S, McGuire AD, Harden JW *et al.* (2009b) Interactions between soil thermal and hydrological dynamics in the response of Alaska ecosystems to fire disturbance. *Journal of Geophysical Research*, **114**, G02015, doi: 10.1029/2008JG000841.
- Yi S, McGuire AD, Kasischke ES, Harden JW, Manies KL, Mack M, Turetsky MR (2010) A dynamic organic soil biogeochemical model for analyzing carbon responses in black spruce forests in interior Alaska. *Journal of Geophysical Research*, doi: 10.1029/2010JG001302.
- Yoshikawa K, Bolton WR, Romanovsky VE, Fukuda M, Hinzman LD (2003) Impacts of wildfire on the permafrost in the boreal forests of interior Alaska. *Journal of Geophysical Research*, **108**, D1, doi: 10.1029/2001JD000438.
- Zhuang Q, McGuire AD, O'Neill KP, Harden JW, Romanovsky VE, Yarie J (2003) Modeling soil thermal and carbon dynamics of a fire chronosequence in interior Alaska. *Journal of Geophysical Research*, **108**, 8147, doi: 10.1029/2001JD001244.

### Supporting Information

Additional Supporting Information may be found in the online version of this article:

**Figure S1.** Map of Alaska (left panel) and study sites across fire chronosequence near Hess Creek (right panel).

**Figure S2.** Sensitivity test to analyze the effect of  $k_{deep}$  and thus turnover time (TT) on deep organic OC stocks.

**Figure S3.** Verification of soil OC accumulation model. (a) Results of model simulation for the first 6500 years since black spruce colonization on the interior Alaskan landscape. (b) Comparison of simulated and measured OC stocks ( $\pm 1$  standard error). Simulated OC stocks reflect the mean during the last fire cycle of the model run.

**Table S1.** Parameters and statistic from linear equations used to predict OC stocks from organic horizon thickness.

Please note: Wiley-Blackwell is not responsible for the content or functionality of any supporting materials supplied by the authors. Any queries (other than missing material) should be directed to the corresponding author for the article.